2014

Dynamic stability analysis for a self-mixing interferometry system

Yuanlong Fan
University of Wollongong, yf555@uowmail.edu.au

Yanguang Yu
University of Wollongong, yanguang@uow.edu.au

Jiangtao Xi
University of Wollongong, jiangtao@uow.edu.au

Qinghua Guo
University of Wollongong, qguo@uow.edu.au

Publication Details

Y. Fan, Y. Yu, J. Xi & Q. Guo, "Dynamic stability analysis for a self-mixing interferometry system," Optics Express, vol. 22, (23) pp. 29260-29269, 2014.

Dynamic stability analysis for a self-mixing interferometry system

Abstract
A self-mixing interferometry (SMI) system is a laser diode (LD) with an external cavity formed by a moving external target. The behavior of an SMI system is governed by the injection current J to the LD and the parameters associated with the external cavity mainly including optical feedback factor C , the initial external cavity length (L0) and the light phase (⌀0) which is mapped to the movement of the target. In this paper, we investigate the dynamic behavior of an SMI system by using the Lang-Kobayashi model. The stability boundary of such system is presented in the plane of (C , ⌀0), from which a critical C (denoted as Ccritical) is derived. Both simulations and experiments show that the stability can be enhanced by increasing either L0 or J . Furthermore, three regions on the plane of (C , ⌀0) are proposed to characterize the behavior of an SMI system, including stable, semi-stable and unstable regions. We found that the existing SMI model is only valid for the stable region, and the semi-stable region has potential applications on sensing and measurement but needs remodeling the system by considering the bandwidth of the detection components.

Disciplines
Engineering | Science and Technology Studies

Publication Details
Y. Fan, Y. Yu, J. Xi & Q. Guo, "Dynamic stability analysis for a self-mixing interferometry system," Optics Express, vol. 22, (23) pp. 29260-29269, 2014.

Dynamic stability analysis for a self-mixing interferometry system

Yuanlong Fan, Yanguang Yu,* Jiangtao Xi and Qinghua Guo

School of Electrical, Computer and Telecommunications Engineering, University of Wollongong, Wollongong, NSW, 2522, Australia

*yanguang@uow.edu.au

Abstract: A self-mixing interferometry (SMI) system is a laser diode (LD) with an external cavity formed by a moving external target. The behavior of an SMI system is governed by the injection current J to the LD and the parameters associated with the external cavity mainly including optical feedback factor C, the initial external cavity length (L_0) and the light phase (ϕ_0) which is mapped to the movement of the target. In this paper, we investigate the dynamic behavior of an SMI system by using the Lang-Kobayashi model. The stability boundary of such system is presented in the plane of (C, ϕ_0), from which a critical C (denoted as $C_{critical}$) is derived. Both simulations and experiments show that the stability can be enhanced by increasing either L_0 or J. Furthermore, three regions on the plane of (C, ϕ_0) are proposed to characterize the behavior of an SMI system, including stable, semi-stable and unstable regions. We found that the existing SMI model is only valid for the stable region, and the semi-stable region has potential applications on sensing and measurement but needs re-modeling the system by considering the bandwidth of the detection components.

OCIS codes: (120.3930) Metrological instrumentation; (120.7280) Vibration analysis; (280.3420) Laser sensors.

References and links

1. N. Servagent, F. Gouaux, and T. Bosch, "Measurements of displacement using the self-mixing interference in a laser diode" J. Opt., **29**, 168 (1998).
2. Y. Yu, X. Qiang, Z. Wei, and X. Sun, "Differential displacement measurement system using laser self-mixing interference effect" Acta Opt. Sin., **19**, 1269-1273 (1999).
3. G. Giuliani, M. Norgia, S. Donati, and T. Bosch, "Laser diode self-mixing technique for sensing applications" J. Opt. A, **4**, S283-S294 (2002).
4. C. Bes, G. Plantier, and T. Bosch, "Displacement measurements using a self-mixing laser diode under moderate feedback" IEEE Trans. Instrum. Meas., **55**, 1101-1105 (2006).
5. Y. Yu, C. Guo, and H. Ye, "Vibration measurement based on moderate optical feedback self-mixing interference" Acta Opt. Sin., **27**, 1430-1434 (2007).
6. M. Norgia, G. Giuliani, and S. Donati, "Absolute distance measurement with improved accuracy using laser diode self-mixing interferometry in a closed loop" IEEE Trans. Instrum. Meas., **56**, 1894-1900 (2007).
7. M. Norgia, A. Pesatori, M. Tanelli, and M. Lovera, "Frequency compensation for a self-mixing interferometer" IEEE Trans. Instrum. Meas., **59**, 1368-1374 (2010).
8. Y. Fan, Y. Yu, J. Xi, and J. F. Chicharo, "Improving the measurement performance for a self-mixing interferometry-based displacement sensing system" Appl. Opt., **50**, 5064-5072 (2011).
9. S. Donati, "Developing self-mixing interferometry for instrumentation and measurements" Laser & Photon. Rev., **6**, 393-417 (2012).
10. A. Magnani, A. Pesatori, and M. Norgia, "Self-mixing vibrometer with real-time digital signal elaboration" Appl. Opt., **51**, 5318-5325 (2012).
11. O. D. Bernal, U. Zabit, and T. Bosch, "Study of laser feedback phase under self-mixing leading to improved phase unwrapping for vibration sensing" IEEE J. Sensors, **13**, 4962-4971 (2013).

12. Y. Yu, G. Giuliani, and S. Donati, "Measurement of the linewidth enhancement factor of semiconductor lasers based on the optical feedback self-mixing effect" IEEE Photon. Techno. Lett., **16**, 990-992 (2004).
13. J. Xi, Y. Yu, J. F. Chicharo, and T. Bosch, "Estimating the parameters of semiconductor lasers based on weak optical feedback self-mixing interferometry" IEEE J. Quantum Electron., **41**, 1058-1064 (2005).
14. Y. Yu, J. Xi, J. F. Chicharo, and T. Bosch, "Toward automatic measurement of the linewidth-enhancement factor using optical feedback self-mixing interferometry with weak optical feedback" IEEE J. Quantum Electron., **43**, 527-534 (2007).
15. L. Wei, J. T. Xi, Y. G. Yu, and J. F. Chicharo, "Linewidth enhancement factor measurement based on optical feedback self-mixing effect: a genetic algorithm approach" J. Opt. A., **11**, 045505 (2009).
16. Y. Yu, and J. Xi, "Influence of external optical feedback on the alpha factor of semiconductor lasers" Opt. Lett., **38**, 1781-1783 (2013).
17. S. Donati, and M. T. Fathi, "Transition from short-to-long cavity and from self-mixing to chaos in a delayed optical feedback laser" IEEE J. Quantum Electron., **48**, 1352-1359 (2012).
18. K. Bertling, Y. L. Lim, T. Taimre, D. Indjin, P. Dean, R. Weih, S. Höfling, M. Kamp, M. von Edlinger, J. Koeth, and A. D. Rakić, "Demonstration of the self-mixing effect in interband cascade lasers" Appl. Phys. Lett., **103**, 231107 (2013).
19. S. Donati and M. Norgia, "Self-mixing interferometry for biomedical signals sensing" IEEE J. Sel. Topics Quantum Electron., **20**, 6900108-6900108 (2014).
20. G. Plantier, C. Bes, and T. Bosch, "Behavioral model of a self-mixing laser diode sensor" IEEE J. Quantum Electron., **41**, 1157-1167 (2005).
21. Y. Yu, J. Xi, J. F. Chicharo, and T. M. Bosch, "Optical feedback self-mixing interferometry with a large feedback factor C: behavior studies" IEEE J. Quantum Electron., **45**, 840-848 (2009).
22. Y. Yu, J. Xi, and J. F. Chicharo, "Measuring the feedback parameter of a semiconductor laser with external optical feedback" Opt. Express, **19**, 9582-9593 (2011).
23. R. Lang, and K. Kobayashi, "External optical feedback effects on semiconductor injection laser properties" IEEE J. Quantum Electron., **16**, 347-355 (1980).
24. J. Mork, B. Tromborg, and J. Mark, "Chaos in semiconductor lasers with optical feedback: theory and experiment" IEEE J. Quantum Electron., **28**, 93-108 (1992).
25. S. Donati, G. Giuliani, and S. Merlo, "Laser diode feedback interferometer for measurement of displacements without ambiguity" IEEE J. Quantum Electron., **31**, 113-119 (1995).
26. W. M. Wang, K. T. V. Grattan, A. W. Palmer, and W. J. O. Boyle, "Self-mixing interference inside a single-mode diode laser for optical sensing applications" IEEE J. Lightwave Techno., **12**, 1577-1587 (1994).
27. T. Taimre, and A. D. Raki, "On the nature of Acket's characteristic parameter C in semiconductor lasers" Appl. Opt., **53**, 1001-1006 (2014).
28. B. Tromborg, J. Osmundsen, and H. Olesen, "Stability analysis for a semiconductor laser in an external cavity" IEEE J. Quantum Electron., **20**, 1023-1032 (1984).
29. S. Merlo, and S. Donati, "Reconstruction of displacement waveforms with a single-channel laser-diode feedback interferometer" IEEE J. Quantum Electron., **33**, 527-531 (1997).
30. H. Li, J. Ye, and J. G. McInerney, "Detailed analysis of coherence collapse in semiconductor lasers" IEEE J. Quantum Electron., **29**, 2421-2432 (1993).
31. S.-Y. Ye, and J. Ohtsubo, "Experimental investigation of stability enhancement in semiconductor lasers with optical feedback" Opt. Rev., **5**, 280-284 (1998).

1. Introduction

Self-Mixing Interferometry (SMI) is an emerging non-contact sensing technique for the measurement of various metrological quantities, such as absolute distance, angle, displacement, and velocity [1-11]. An SMI system is composed of a laser diode (LD) with a photodiode (PD) packaged at the rear of the LD, a lens, an external target and a data processing unit. When the external target moves, a small portion of light reflected re-enters the internal cavity of the LD, leading to the modulation in both the amplitude and frequency of the LD output power. The modulated power is detected by the PD as an SMI signal, which is fed to the data processing unit for extracting useful information related to both the external target and the LD itself [12-16]. In contrast to the traditional interferometric sensing techniques, the SMI is advantageous by impact structure, low-cost and simple implementation, thus attracted intensive research [9, 17-19] in recent years.

In the above-mentioned applications, it is desired that an SMI system operates in a stable mode, in which case the LD biased by constant injection current usually leads to SMI signals with symmetric sinusoidal-like fringes or asymmetric sawtooth-like fringes, depending on the external optical feedback level. The feedback level is measured by a factor *C* defined in

[20-22]. However, with the change of operational conditions, such as injection current and parameters associated with the external cavity including C and external cavity length, the LD can also exhibit unstable behavior. In this case, an SMI system will degrade or even lose its sensing ability. Therefore it is very important to investigate the stability of an SMI system with respect to its operational conditions.

An SMI system is an LD with a time varying external cavity. Its dynamic behavior can be described by the well known Lang and Kobayashi (L-K) equations [23] as follows:

$$\frac{dE(\mathrm{t})}{dt}=\frac{1}{2}\left\{G\left[N(t),E(t)\right]-\frac{1}{\tau_p}\right\}E(t)+\frac{\kappa}{\tau_{in}}\cdot E(t-\tau)\cdot\cos\left[\omega_0\tau+\phi(t)-\phi(t-\tau)\right] \quad (1)$$

$$\frac{d\phi(\mathrm{t})}{dt}=\frac{1}{2}\alpha\left\{G\left[N(t),E(t)\right]-\frac{1}{\tau_p}\right\}-\frac{\kappa}{\tau_{in}}\cdot\frac{E(t-\tau)}{E(t)}\cdot\sin\left[\omega_0\tau+\phi(t)-\phi(t-\tau)\right] \quad (2)$$

$$\frac{dN(\mathrm{t})}{dt}=\frac{J}{eV}-\frac{N(t)}{\tau_s}-G\left[N(t),E(t)\right]E^2(t) \quad (3)$$

where $E(t)$, $\phi(t)$ and $N(t)$ are respectively electric field amplitude, electric field phase and carrier density. t is the time index. $\phi(t)$ is given by $\phi(t)=\left[\omega(t)-\omega_0\right]t$, where $\omega(t)$ and ω_0 are the optical angular frequency for an LD with and without feedback respectively. The dynamics of the system are governed by the injection current (J) to the LD and the parameters associated to the external cavity including the feedback strength (κ) and the external cavity round-trip time of the light (τ). $\kappa=(1-r_1^2)r_2/r_1$, where r_1 and r_2 are the reflectivity of the LD's front facet and the external target respectively. $\tau=2L/c$, where L is the external cavity length and c is the speed of light. The other parameters in Eqs. (1)-(3) are related to the solitary LD itself and are treated as constants for a certain LD and these parameters are defined in Table 1 [24]. As LD vendors normally do not provide the values for these parameters, we just adopted their values from [24] for the below simulation analysis.

Table 1. Physical meanings for the internal cavity parameters in L-K equations [24]

Symbol	Physical Meaning	Value
G_N	modal gain coefficient	$8.1\times10^{-13}m^3s^{-1}$
N_0	carrier density at transparency	$1.1\times10^{24}m^{-3}$
ε	nonlinear gain compression coefficient	$2.5\times10^{-23}m^3$
Γ	confinement factor	0.3
τ_p	photon life time	$2.0\times10^{-12}s$
τ_{in}	internal cavity round-trip time	$8.0\times10^{-12}s$
α	line-width enhancement factor	6.0
e	elementary charge	$1.6\times10^{-19}C$
V	volume of the active region	$1.0\times10^{-16}m^3$
τ_s	carrier life time	$2.0\times10^{-9}s$

The existing SMI model is derived from the stationary solutions of the above L-K equations. Let E_s, N_s and ω_s represent the stationary solutions of L-K equations for electric field amplitude, carrier density and angular frequency respectively. When the system described by Eqs. (1)-(3) enters into a stationary state, we have $dE(t)/dt=0$, $d\phi(t)/dt=\omega_s-\omega_0$ and $dN(t)/dt=0$. Substituting $E(t)=E(t-\tau)=E_s$, $N(t)=N_s$,

$\phi(t) = (\omega_s - \omega_0)t$ and $\phi(t-\tau) = (\omega_s - \omega_0)(t-\tau)$ into Eqs. (1)-(3). The well known stationary solutions can be obtained as below [3, 9, 17, 20, 23, 24]:

$$\omega_0 \tau = \omega_s \tau + \frac{\kappa}{\tau_{in}} \tau \sqrt{1+\alpha^2} \sin(\omega_s \tau + \arctan \alpha) \tag{4}$$

$$N_s = N_0 + \frac{1}{\tau_p G_N} - \frac{2\kappa \cos(\omega_s \tau)}{\tau_{in} G_N} \tag{5}$$

$$E_s^2 = \frac{J/(\mathrm{eV}) - N_s/\tau_s}{G_N (N_s - N_0)} \tag{6}$$

Note that α in Eq. (4) is a very important factor as its value describes many aspects of the laser behaviour, such as spectral effects, injection locking and the modulation response [12, 14-16].

From Eqs. (4)-(6) by considering a moving target, the existing SMI model can be obtained as below by introducing:

$$\phi_0 = \omega_0 \tau,\ \phi_s = \omega_s \tau \text{ and } C = \frac{\kappa}{\tau_{in}} \tau \sqrt{1+\alpha^2} \tag{7}$$

Then Eq. (4) becomes:

$$\phi_0 = \phi_s + C \sin(\phi_s + \arctan \alpha) \tag{8}$$

Equation (8) is called the phase equation, where ϕ_0 and ϕ_s are the light phase without and with feedback respectively. C is referred to as the optical feedback factor. By substituting Eq. (5) into Eq. (6), the normalized variation of the LD output power (that is the so called SMI signal g) can be described as [25]:

$$g = \cos(\phi_s) \tag{9}$$

Equations (8) and (9) are the existing SMI model which has been widely accepted to describe the waveforms of SMI signals [1-16, 20-22, 25]. In the SMI model, C is an important parameter as it characterizes the waveform of an SMI signal. When $C < 1$, equation (8) presents an unique mapping from ϕ_0 and ϕ_s. In this situation, the SMI signal contains sinusoidal-like fringes. For $C > 1$, equation (8) may yield multiple possible ϕ_s, and the SMI signal shows asymmetric hysteresis and produces sawtooth-like fringes. The mechanism of generating an SMI signal as well as its behavior with respect to C has been well-established and presented in [8, 20, 21, 26, 27].

However, when the system enters into the unstable state, the premise for deriving the stationary solutions will be no longer valid, thus leading to the actual behavior of the system can not be described by the existing SMI model. In this paper, the stability boundary of an SMI system is obtained and presented in a two dimensional plane defined by C and ϕ_0. By studying the features of the boundary, a critical C (denoted as $C_{critical}$) is derived. If only an SMI system is designed with a feedback level below $C_{critical}$, its sensing performance can be guaranteed and the behavior of the system can be described by the existing SMI model, otherwise by the L-K model. An experimental method for determining the $C_{critical}$ is presented. The influence of the initial external cavity length and the injection current on the $C_{critical}$ are investigated from both simulations and experiments.

2. Stability boundary of an SMI system

The stable condition for an LD containing an external cavity was previously derived by [24, 28] based on L-K equations, as shown below:

$$-\alpha\kappa\sin(\phi_s)+\kappa\cos(\phi_s)\left[1-2\left(\frac{\Omega}{\omega_R}\right)^2\right]<\left(\frac{\Omega}{\omega_R}\right)^2\frac{\tau_{in}}{2\tau_R\sin^2(\Omega\tau_0/2)} \tag{10}$$

for all the values of Ω (Ω is defined as the imaginary part for a complex number in Laplace transform domain. The details can be found in [24, 28]), satisfying:

$$\Omega^2-\omega_R^2=\frac{\Omega}{\tau_R}\cot(\frac{\Omega\tau_0}{2}) \tag{11}$$

where

$$\omega_R=\sqrt{\frac{G_N}{\tau_p}E_{s0}}\ ,\ \frac{1}{\tau_R}=\frac{1}{\tau_s}+\left(\tau_p+\frac{\varepsilon\Gamma}{G_N}\right)\omega_R^2 \tag{12}$$

In Eqs. (11) and (12), E_{s0} is the stationary electric field amplitude of the solitary laser which is determined by the injection current J [28]. ω_R and τ_R are called the relaxation oscillation frequency and the damping time of the solitary laser [24]. τ_0 is the initial external cavity round-trip time of the light, i.e., $\tau_0=2L_0/c$, where L_0 is the initial external cavity length.

When designing an SMI system, it is important to know how to configure the system in terms of a proper feedback level and suitable movement range for the external target. That is, we need to know the stable boundary for the parameter C and the phase ϕ_0. Hence, we propose to describe the stability of an SMI system in the plane of (C, ϕ_0). To achieve this, let us replace κ by C (via $C=\frac{\kappa}{\tau_{in}}\tau_0\sqrt{1+\alpha^2}$) in the stable condition described by Eq. (10). Note that the amount of movement of target should be much smaller than the initial external cavity length. Then, equation (10) can be written as:

$$C\left\{\cos(\phi_s)\left[1-2\left(\frac{\Omega}{\omega_R}\right)^2\right]-\alpha\sin(\phi_s)\right\}\le\left(\frac{\Omega}{\omega_R}\right)^2\frac{\tau_0\sqrt{1+\alpha^2}}{2\tau_R\sin^2(\Omega\tau_0/2)} \tag{13}$$

where the equal sign corresponds to the condition of stability boundary. What we want is to work out the relationship between C and ϕ_0 to describe the stability for an SMI system. Let us consider the parameters appeared in Eq. (13). Generally, α is treated as a constant with the value from 3 to 6 [25, 29]. ϕ_s is the dependent variable of ϕ_0, which can be determined by Eq. (8). Both ω_R and τ_R are dependent on the injection current J according to Eq. (12) via E_{s0} [24, 28]. Ω is determined by J and τ_0 according to Eq. (11). So we can say, in Eqs. (13) and (11), J and τ_0 are two governing parameters that determine the stability boundary of an SMI system described by C and ϕ_0. Therefore, it is very important to investigate how the two parameters influence the stability boundary.

In order to work out the stability boundaries in the plane of (C, ϕ_0), we vary ϕ_0 from -3π to 3π and C from 0 to 6 respectively with an interval of 0.015π and 0.015, and for every pair of (C, ϕ_0) we solve Eq. (13) together with Eqs. (11) and (8). The result of the stability boundaries can be obtained in Fig. 1 under different values for the parameter pairs of

J and τ_0. As τ_0 is associated to L_0 via $\tau_0 = 2L_0/c$, instead of τ_0, we present the influence of L_0 on the stability boundary in order to provide a more informative physical meaning related to the SMI system. In Fig. 1(a), the boundary is computed with three different J for a fixed $L_0 = 0.25m$. In Fig. 1(b), the boundary is computed with three different L_0 for a fixed $J = 1.3J_{th}$, where J_{th} is the threshold injection current. The area below each boundary is the stable region. In Fig. 1, we also indicate the different feedback regimes defined by the value of C, where weak feedback regime is for $C < 1$, moderate feedback regime for $1 < C < 4.6$ and strong feedback regime for $C > 4.6$ [21].

From Fig. 1, the following features of the stability boundary can be found:

1. The stability boundary shows periodic fluctuation with a period of 2π equivalent to a half wavelength movement of the external cavity.
2. The system is always stable at a weak feedback regime and may enter unstable when the feedback level is moderate or high feedback regime.
3. To achieve a stable status at a moderate or high feedback regime, we can either increase the injection current or choose a long external cavity.

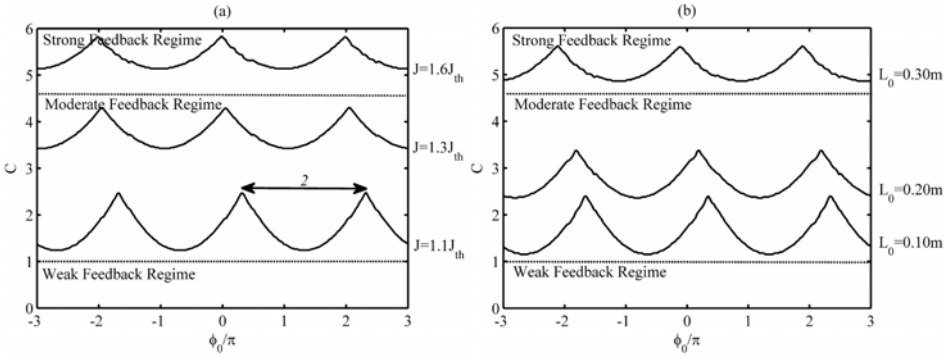

Fig. 1. Influence of J and L_0 on the stability boundary of an SMI system. (a) for a fixed $L_0 = 0.25m$ with different J, (b) for a fixed $J = 1.3J_{th}$ with different L_0.

Figure 2 shows a boundary when $J = 1.1J_{th}$ and $L_0 = 0.35m$. In Fig. 2, we define three different regions referred to as stable, semi-stable and unstable respectively according to the dynamic behavior of an SMI system described as below. As the existing SMI model described in Eqs. (8) and (9) is not able to describe the actual behavior of an SMI system when the system enters the region above the stability boundary, we need to start from L-K equations to investigate the output power of an SMI system, i.e., $E^2(t)$. The calculation of $E^2(t)$ by the L-K equations uses the 4-th order Runge-Kutta integration algorithm.

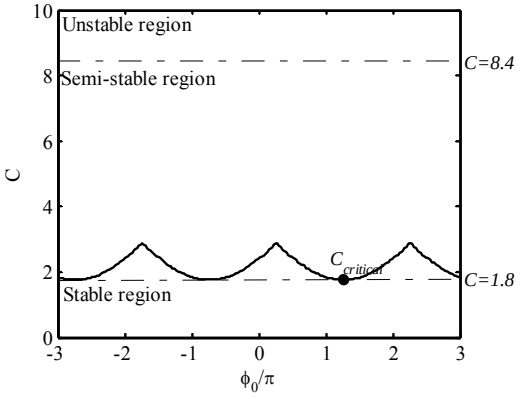

Fig. 2. The stability boundary of an SMI system when $J = 1.1J_{th}$ and $L_0 = 0.35m$.

Now, let us study the features of the LD output power (below we will call it as an SMI signal) obtained by the L-K model at the different region defined in Fig. 2. We choose $C = 1.5$, $C = 2.5$, $C = 4.0$ and $C = 9.0$ which respectively correspond to the stable, semi-stable, semi-stable and unstable regions. Other parameters in the L-K model take the values shown in Table 1. The SMI signal $g(t)$ is calculated as the normalized $E^2(t)$. Supposing that the external target moves at a sinusoidal law with $L(t) = L_0 + \Delta L \cdot \sin(2\pi ft)$, where ΔL and f are the vibration amplitude and frequency respectively which are chosen as $\Delta L = 1.17\mu m$ and $f = 75Hz$, for the purpose of comparison, Fig. 3 presents the SMI signals predicted respectively by the L-K model shown from Figs. 3(b)-3(e) and the existing SMI model from Figs. 3(g)-3(j). In each row of Fig. 3, the two SMI signals are obtained under the same operation condition, i.e., the same C value.

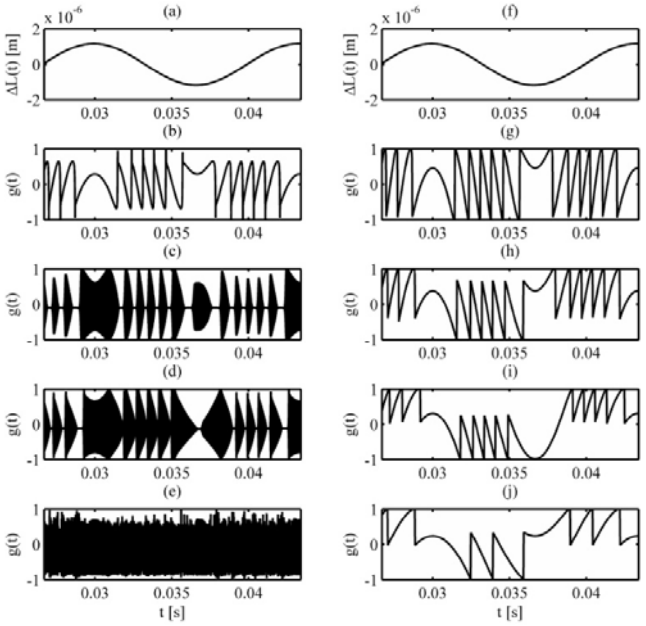

Fig. 3. SMI signals predicated by the L-K model and the existing SMI model respectively. (a) and (f): movement trace of the external target, (b)-(e): SMI signals obtained by the L-K model with $C = 1.5$, $C = 2.5$, $C = 4.0$ and

$C = 9.0$ respectively. (g)-(j) SMI signals obtained by the existing SMI model with $C = 1.5$, $C = 2.5$, $C = 4.0$ and $C = 9.0$ respectively.

According to the L-K model, obviously, only Fig. 3(b) with $C = 1.5$ shows a stable SMI signal which can also be described by using the existing SMI model shown in Fig. 3(g). $C = 1.5$ indicates the SMI system is stable in Fig. 2. In the region with $1.8 < C < 8.4$, simulations using the L-K model shows that the SMI signal contains a high frequency oscillation close to the relaxation oscillation frequency of the solitary laser. Figures 3(c) and 3(d) give the two SMI signals at the semi-stable region, which are more complicated than Fig. 3(b). Hence, the behaviors described by the L-K model are different from the ones by the existing SMI model resulting from the stationary solutions of the L-K model. It is very interesting to observe that, even for a complicated waveform shown in Figs. 3(c) and 3(d), the movement information of the target is still visible. This is why we call the region $1.8 < C < 8.4$ as the semi-stable region. With the aid of signal processing technology, the system operating at the semi-stable region can also be used for sensing and measurement. In order to achieve this, the SMI waveform needs to be investigated to reveal its relationship to the movement of the target. Also, due to the limit in the rising time of the PD packaged at the rear of the LD, it may not be able to detect the details of the high frequency SMI waveform in the semi-stable region, and the SMI signal observed will be a distorted version of the high frequency waveform. A complete theoretical model is required to describe the influence of the limited bandwidth of the PD on the high frequency SMI waveform with the aim to detect the movement of the target from the distorted SMI waveform. Obviously, extensive work is required and could be an interesting topic for future research. When $C > 8.4$, it is hard to see the vibration information from the SMI waveform, implying that the SMI system may lose its sensing ability. In this situation, the spectrum of laser is dramatically broadened, which is beyond the scope of this paper. Fig. 3(e) shows the SMI signal with $C = 9$ indicating that the SMI system is not suitable for sensing applications.

Note that the SMI model is derived from the L-K model by letting $dE(t)/dt = 0$, $d\phi(t)/dt = \omega_s - \omega_0$ and $dN(t)/dt = 0$. These conditions will no longer be valid when the system enters semi-stable or unstable region, e.g., the relaxation oscillation will become undamped [30, 31]. In summary, for the system working in the semi-stable or unstable region, the existing SMI model cannot be used, but we can still use the fundamental L-K model to describe the system behaviour.

Furthermore, from the stability boundary shown in Figs. 1 and 2, We noticed that from the stability boundary a critical C (denoted by $C_{critical}$) can be defined under which the system is guaranteed to be stable. As $C_{critical}$ corresponds to the bottom on the stability boundary, by performing differentiation with respect to ϕ_0 on both sided of Eq. (13), we can obtain ϕ_s for $C = C_{critical}$ as follows:

$$\phi_s = \arctan\left[\frac{\alpha}{2\left(\Omega/\omega_R\right)^2 - 1}\right] + p\pi \tag{14}$$

where p denotes an integer. As $C_{critical}$ lies on the stability boundary described by Eq. (13), inserting Eq. (14) into Eq. (13), thus we can obtain:

$$C_{critical} = \left(\frac{\Omega}{\omega_R}\right)^2 \frac{L_0\sqrt{1+\alpha^2}}{\tau_R c \sin^2\left(\Omega L_0/c\right)} \frac{\sqrt{\left[2\left(\Omega/\omega_R\right)^2 - 1\right]^2 + \alpha^2}}{\left[2\left(\Omega/\omega_R\right)^2 - 1\right]^2 + \alpha^2} \tag{15}$$

for all the values of Ω satisfying Eq. (11). Equation (15) can be used to estimate $C_{critical}$ when designing an SMI system if the values of the parameters listed in Table 1 are available.

3. Experiment

In this section, we present a experimental method to determine $C_{critical}$, and investigate how L_0 and J influence $C_{critical}$. Figure 4 shows the experimental SMI setup for such investigation. A $0.8\mu m$ band single mode GaAlAs triple quantum well LD (HL8325G) from Hitachi was employed in the experiments. The temperature of the LD was stabilized to within $0.01^0 C$ by using a temperature controller (model TED200). The injection current to the LD was controlled by a laser diode controller (model LDC2000). The light emitted from the LD was focused by a lens and split into two beams by a beam splitter (BS). One beam was directed to the external target and then was reflected back to the LD internal cavity. The other beam was collected by an optical spectrum analyzer (Advantest Q8347) for monitoring the optical spectrum of the SMI system. A piece of mirror was attached on the surface of a loudspeaker so that to achieve a strong optical feedback level. The loudspeaker was driven by a sinusoidal signal with 75Hz generated by a signal generator. The optical feedback level of the SMI system was adjusted by an attenuator inserted in between the BS and the loudspeaker. The SMI signal was detected by the PD packaged at the rear of the LD, then collected by data acquisition device and finally processed by the data processing unit.

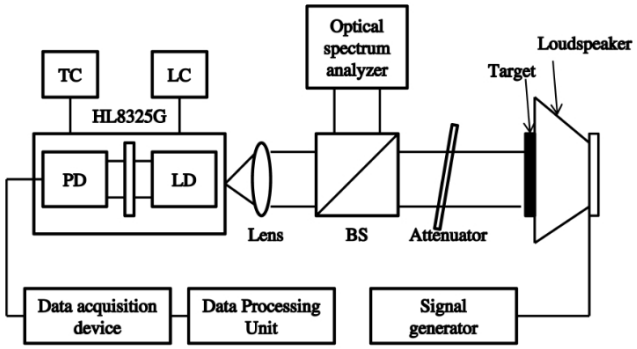

Fig. 4. Experimental setup for investigating the influence of the external cavity length and the injection current respectively on the critical feedback level

When the SMI system is in the stable region, the observed optical spectrum is clean showing the LD operating on only one single mode as shown in Fig. 5(a). When the system enters into semi-stable region, the relaxation oscillation of the laser becomes undamped. In this case, a subpeak corresponding to the relaxation oscillation frequency appears near to the main peak of the optical spectrum [30, 31]. Figure 5(b) shows the optical spectrum observed when the system in the semi-stable region. As our spectrum analyzer has a relative low resolution with 0.002nm, it is not able to separate clearly the subpeak from the mean peak. However, it can still tell us the appearance of the relaxation oscillation of the laser with frequency about 2-4GHz, therefore determining the stability of the system changes from stable to semi-stable.

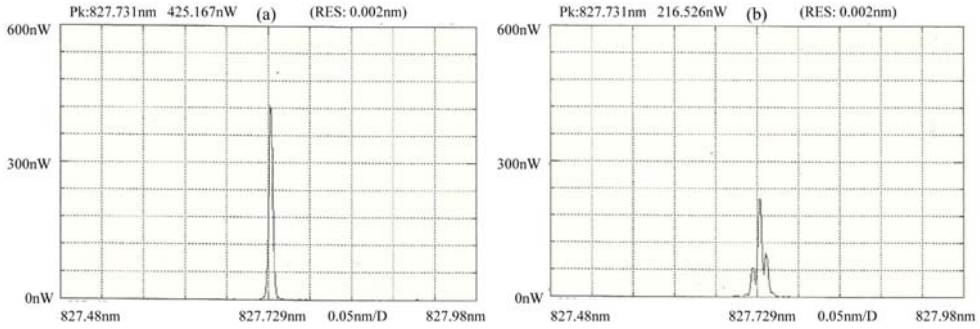

Fig. 5. Two optical spectra obtained with $L_0 = 0.25m$ and $J = 1.7J_{th}$ for (a) the stable region, (b) the semi-stable region.

In the following experiments, we varied the feedback level from weak to strong with the aid of the attenuator, the single mode spectrum displayed on the spectrum analyzer will thus change. Once the subpeaks was first observed from the spectrum, the SMI system should be at the point of the critically stable. Then, we apply a tiny change to the attenuator by reversely rotating it 2 degrees. A stable SMI signal very close to the critical level can thus be obtained and we used the signal to calculate the parameter C by the method presented in [16]. The C calculated is approximately represented for $C_{critical}$.

Based on above experimental method for estimating $C_{critical}$, the influence of J and L_0 respectively on the $C_{critical}$ are also investigated. Figure 6 (a) shows the $C_{critical}$ goes up with the increase of the injection current for a fixed $L_0 = 0.25m$. Figure 6 (b) shows the longer the external cavity the higher $C_{critical}$ for a fixed $J = 1.3J_{th}$. Obviously, the experimental results show the same trend with the simulation analysis shown in Fig. 1 and 2, that is, $C_{critical}$ can be increased by either increase of J or L_0, thus leading to stability enhancement of the SMI system. We note that the experimental results obtained do not exactly agree with simulations. The reason is that the actual values of the internal parameters for the LD used in the experiment are different from the parameters shown in Table 1 for the simulation.

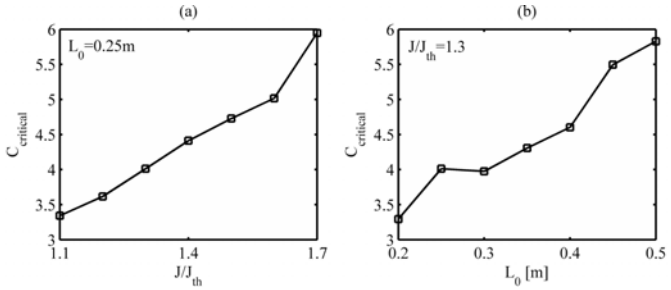

Fig. 6. Experimental results. (a) for a fixed $L_0 = 0.25m$, (b) for a fixed $J/J_{th} = 1.3$.

4. Conclusion

The stability of an SMI system is investigated in this paper. It is found that, to achieve a stable SMI signal for sensing purpose under moderate or strong feedback level, we can either increase the initial external cavity length or the injection current to the laser. By monitoring the spectrum of the SMI system, a critical optical feedback factor $C_{critical}$ can be determined

approximately. Under the $C_{critical}$, an SMI system is guaranteed to be stable and the existing SMI model can exactly describe the waveform of an SMI signal. Furthermore, we presented another two regions on the plane of (C, ϕ_0) called semi-stable and unstable with boundaries corresponding to the undamped relaxation oscillation and the chaos status respectively. We found that semi-stable region has potential applications on sensing and measurement but may require further signal processing technology. The results presented in this paper provide useful guidance for designing various SMI based sensing and instrumentations.